

SUPPLEMENTARY MATERIAL

Ab-initio modelling of hydrogen molecular rotation in the outside of carbon nanotubes

María Pilar de Lara-Castells^a and Alexander O. Mitrushchenkov^b

^a Instituto de Física Fundamental (C.S.I.C.), Serrano 123, E-28006, Madrid, Spain;

^b Université Paris-Est, Laboratoire Modélisation et Simulation Multi Echelle, MSME UMR 8208, CNRS, UPEC, UPEM, F-77454, Marne la Vallée, France

ARTICLE HISTORY

Compiled November 28, 2018

In Table 1 we analyze the contribution of individual V^{ik} terms to the energy of different rotational levels, corresponding to

$$(1 - x^2)^i \cos^{2k}(\phi) = \sin^{2i}(\theta) \cos^{2k}(\phi),$$

cf. Eq. (6) of the main manuscript. From Table 1, it can be observed that the terms with $i > 1$ can be safely neglected. Hence, the main contribution comes from the V^{00} , V^{10} and V^{11} components. For convenience, they can be written in terms of the full three-dimensional (3D) interaction potential at specific values of the angles θ and ϕ :

$$V^{00}(R) = V(R, \theta = 0^\circ, \phi = \text{any})$$

$$V^{10}(R) = V(R, \theta = 90^\circ, \phi = 90^\circ) - V(R, \theta = 0^\circ, \phi = \text{any})$$

$$V^{11}(R) = V(R, \theta = 90^\circ, \phi = 0^\circ) - V(R, \theta = 90^\circ, \phi = 90^\circ)$$

Assuming that j is a good quantum number, we have to evaluate the angular factors over spherical harmonics. It is reminded that we employ

$$\Theta_{j|m|}(\theta) \frac{\exp(im\phi)}{\sqrt{2\pi}}$$

as a basis, which differs from spherical harmonics only by a phase factor for $m < 0$. Due to the symmetry of the problem, we further symmetrize functions of ϕ for $m \neq 0$ such as $|+m\rangle \equiv \cos(m\phi)/\sqrt{\pi}$ and $|-m\rangle \equiv \sin(m\phi)/\sqrt{\pi}$, which are then equivalent to real spherical harmonics.

Table 1. Decomposition of the dispersion and dispersionless contributions of the potential for different rotational energy levels as a function of i and k (see also Table 2 of the main manuscript). Energies E are given in cm^{-1} being relative to those of the ground state. The contribution of kinetic energy terms is also given for comparison.

		CNT(10,10)		CNT(5,5)	
i	k	Disp	Disp-less	Disp	Disp-less
$j = 0, m = 0$					
$E = 0, \langle V \rangle = -289.5, \langle K_R \rangle = 28.7$			$E = 0, \langle V \rangle = -214.4, \langle K_R \rangle = 24.6$		
$\langle K_{int} \rangle = 0.399, \langle K_{ext} \rangle = 0.0003$			$\langle K_{int} \rangle = 1.45, \langle K_{ext} \rangle = 0.0019$		
0	0	-510.0	231.5	-397.4	214.8
1	0	3.1	0.0	3.5	-11.1
1	1	-27.6	13.9	-21.5	2.4
2	0	0.0	0.0	0.0	0.0
2	1	0.3	0.0	0.4	0.0
2	2	-0.8	0.0	-0.7	0.0
$j = 1, m = 0$					
$E = 123.1, \langle V \rangle = -284.5, \langle K_R \rangle = 28.3$			$E = 131.0, \langle V \rangle = -199.2, \langle K_R \rangle = 22.7$		
$\langle K_{int} \rangle = 118.8, \langle K_{ext} \rangle = 0.000$			$\langle K_{int} \rangle = 119.1, \langle K_{ext} \rangle = 0.000$		
0	0	-512.5	234.3	-384.8	203.2
1	0	1.9	0.0	2.0	-6.3
1	1	-16.2	8.2	-11.7	-1.5
2	0	0.0	0.0	0.0	0.0
2	1	0.1	0.0	0.1	0.0
2	2	-0.3	0.0	-0.3	0.0
$j = 1, m = +1$					
$E = 108.7, \langle V \rangle = -300.1, \langle K_R \rangle = 29.5$			$E = 100.4, \langle V \rangle = -234.5, \langle K_R \rangle = 27.0$		
$\langle K_{int} \rangle = 118.9, \langle K_{ext} \rangle = 0.081$			$\langle K_{int} \rangle = 119.3, \langle K_{ext} \rangle = 0.178$		
0	0	-508.0	228.9	-409.1	225.4
1	0	3.7	0.0	4.3	-13.5
1	1	-47.4	23.7	-36.9	-3.8
2	0	0.0	0.0	0.0	0.0
2	1	0.6	0.0	0.7	0.0
2	2	-1.6	0.0	-1.5	0.0
$j = 1, m = -1$					
$E = 125.1, \langle V \rangle = -282.4, \langle K_R \rangle = 28.2$			$E = 127.1, \langle V \rangle = -203.8, \langle K_R \rangle = 23.2$		
$\langle K_{int} \rangle = 118.8, \langle K_{ext} \rangle = 0.081$			$\langle K_{int} \rangle = 119.1, \langle K_{ext} \rangle = 0.176$		
0	0	-509.8	231.7	-392.7	211.0
1	0	3.7	0.0	4.1	-12.7
1	1	-16.1	8.1	-12.0	-1.4
2	0	0.0	0.0	0.0	0.0
2	1	0.2	0.0	0.2	0.0
2	2	-0.3	0.0	-0.3	0.0

The explicit evaluation of angular factors provides the following relationship

$$\langle \Theta_{jm} | 1 - x^2 | \Theta_{jm} \rangle = \frac{1}{2j+1} \left\{ \frac{(j-m)(j-m-1)}{2j-1} + \frac{(j+m+1)(j+m+2)}{2j+3} \right\}$$

for θ and

$$\langle \pm m | \cos^2(\phi) | \pm m \rangle = \frac{1}{2}$$

with the exception of $\langle +1 | \cos^2(\phi) | +1 \rangle = 3/4$ and $\langle -1 | \cos^2(\phi) | -1 \rangle = 1/4$. For $j > 1$ there are also couplings for $\Delta m=2$:

$$\langle \pm m | \cos^2(\phi) | \pm (m \pm 2) \rangle = \frac{1}{4}$$

with $\langle 0 | \cos^2(\phi) | +2 \rangle = 1/2\sqrt{2}$. The corresponding factors for θ can also be easily evaluated using recurrence relations. For instance, the explicit expression for $j = 2$ is:

$$\langle \Theta_{20} | 1 - x^2 | \Theta_{22} \rangle = -\frac{4}{7} \sqrt{\frac{2}{3}}$$

Using these expressions, we can readily write effective diagonal one-dimensional (1D) potentials as

$$V_{jm}(R) = V^{00}(R) + q_{10}V^{10}(R) + q_{11}V^{11}(R)$$

Explicit expressions of the coefficients q_{10} and q_{11} for $j \leq 2$ are presented in Table 2.

Table 2. Explicit expressions of the coefficients q_{10} and q_{11} for $j \leq 2$.

j	m	q_{10}	q_{11}
0	0	$\frac{2}{3}$	$\frac{1}{3}$
1	0	$\frac{3}{5}$	$\frac{2}{5}$
1	+1	$\frac{4}{5}$	$\frac{3}{5}$
1	-1	$\frac{4}{5}$	$\frac{1}{5}$
2	0	$\frac{10}{21}$	$\frac{5}{21}$
2	+1	$\frac{4}{7}$	$\frac{3}{7}$
2	-1	$\frac{4}{7}$	$\frac{1}{7}$
2	+2	$\frac{6}{7}$	$\frac{3}{7}$
2	-2	$\frac{6}{7}$	$\frac{3}{7}$

Aimed to provide deeper physical insights, we present the explicit expressions of the potentials for $j \leq 1$ in terms of the three-dimensional (3D) interaction potentials

at different angular configurations as,

$$\begin{aligned}
V_{j=0}(R) &= \frac{1}{3} \{V(R, \theta = 0^\circ) + V(R, \theta = 90^\circ, \phi = 0^\circ) + V(R, \theta = 90^\circ, \phi = 90^\circ)\} \\
V_{j=1, m=0}(R) &= \frac{1}{5} \{3V(R, \theta = 0^\circ) + V(R, \theta = 90^\circ, \phi = 0^\circ) + V(R, \theta = 90^\circ, \phi = 90^\circ)\} \\
V_{j=1, m=+1}(R) &= \frac{1}{5} \{V(R, \theta = 0^\circ) + 3V(R, \theta = 90^\circ, \phi = 0^\circ) + V(R, \theta = 90^\circ, \phi = 90^\circ)\} \\
V_{j=1, m=-1}(R) &= \frac{1}{5} \{V(R, \theta = 0^\circ) + V(R, \theta = 90^\circ, \phi = 0^\circ) + 3V(R, \theta = 90^\circ, \phi = 90^\circ)\}
\end{aligned}$$

which perfectly match the orientations of the corresponding wave functions as isotropic, along Z ($\theta = 0$), X ($\theta = 90^\circ, \phi = 0^\circ$), and Y ($\theta = 90^\circ, \phi = 90^\circ$). The effective potentials are shown in Figures 1 and 2.

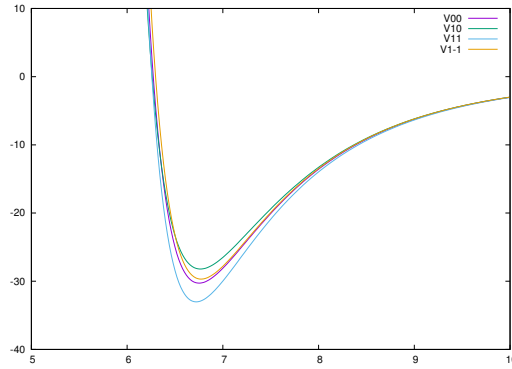


Figure 1. Effective 1D potentials for $j = 0$ and $j = 1$ for H_2 in the outside of the CNT(5,5) nanotube.

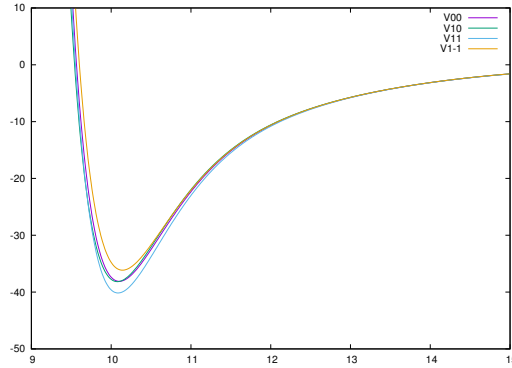


Figure 2. Effective 1D potentials for $j = 0$ and $j = 1$ for H_2 in the outside of the CNT(10,10) nanotube.

The energy levels within this effective 1D model for $\Lambda = 0$ can be obtained by diagonalizing an effective 1D Hamiltonian to which the internal rotational energy should be added,

$$\hat{H}_{jm}^{\text{eff}}(R) = \hat{K}(R) + V_{jm}(R) + j(j+1) B_{H_2}$$

We notice that for $j > 1$, as mentioned above, off-diagonal potential coupling terms might show up, coming from the V_{11} term. For example, for $j = 2$, the following coupling term is non-zero:

$$\langle 20|\hat{H}|2+2\rangle = -\frac{2}{7\sqrt{3}}V^{11}$$

In this case, the combined multi-channel Hamiltonian is constructed and diagonalized, increasing the size of the problem. This simple 1D model is capable of accurately reproducing the energy levels obtained with the full three-dimensional (3D) treatment, as clearly shown in Table 2 of the main manuscript.

Focusing on the levels with $j = 2$, we can observe an interesting feature in Table 2 of the main manuscript: the sub-levels $m = 0$ and $m = -1$ are nearly degenerate for both (5,5) and (10,10) CNTs while the energies of the levels with $m = -2$ and $m = +1$ are very close. At first glance, this could look surprising since the level $m = 0$ is obtained via simultaneous diagonalization of the $m = 0$ and $+2$ basis functions. This can be easily understood when assuming that the V_{10} contribution is smaller than the V_{11} contribution. This condition becomes exact for a CNT with infinite diameter (i.e., for the graphene limit). Then, we could first diagonalize the (2×2) potential matrix (i.e., V_{11}). This operation would result in a $\pi/6$ rotation of the $m = 0, +2$ basis functions, with the eigenvalue of the q_{11} matrix being equal to $1/7$ for $m = 0$ (and to $11/21$ for $m = +2$). Then, as shown in Table 2 above, the q_{11} effective values are the same ($1/7$) for $m = 0$ and $m = -1$. The same holds true for the levels with $m = -2$ and $m = 1$ ($3/7$). Moreover, the transformed coefficient q_{10} becomes the same also for $m = 0$ and $m = -1$ ($4/7$), which explains why these levels are nearly exactly degenerate even for the (5,5) CNT. This q_{10} coefficient is different for $m = -2$ and $m = 1$, resulting in a slight splitting. We must surely note that this diagonalization introduces off-diagonal kinetic terms, mainly due to the K_R kinetic energy term. However, the values of these off-diagonal matrix elements are very small (proportional to the diagonal difference of K_R values, see Table 1 above, i.e. $1-2 \text{ cm}^{-1}$) and can be neglected. It should be also noticed that in the limit of infinite diameter, i.e. the graphene limit, and considering the change of quantization axes, this corresponds to an exact degeneracy of $\pm m$ levels. In fact, by considering the explicit expressions of spherical Harmonics in CNT-like and graphene-like coordinates, we can show that: (1) $m = -2, 1$ levels of CNT correspond to $m = +1, -1$ levels in graphene; (2) the $\pi/6$ rotated $m = 0$ and $m = -1$ levels of CNT correlate with the $m = +2, -2$ levels of graphene; (3) and the $\pi/6$ rotated $m = +2$ level of CNT corresponds to the $m = 0$ level of graphene. This explains why the levels with $j = 2$ behave similarly to those obtained in the case of graphene, where the splittings are proportional to m^2 when the graphene coordinate system is used instead [1].

References

- [1] M. P. de Lara-Castells and A. O. Mitrushchenkov, *J. Phys. Chem. A*, 2015, **119**, 11022–11032.